Line Width Narrowing with ^{14}N Nuclear Quadrupole Resonance Lines at 296 K and 77 K Using a High Powered Pulsed Spectrometer*

R. J. Trepanier and M. A. Whitehead
Department of Chemistry, McGill University, Montréal, Québec, Canada

Z. Naturforsch. **41 a**, 386–391 (1986); revised version received November 25, 1985

The dependence of the NQR line width on the RF pulse intensity and period using a continuous steady state pulse train for polycrystalline ^{14}N compounds shows a dependence on the asymmetry parameter η, the temperature, and the crystal structure.

Introduction

Mechanisms which determine the line shape $g(\nu)$ and line width Δl in NQR studies are:

(i) the time the excess population of high state spins takes to reach the Boltzman equilibrium after NQR excitation, the *spin-lattice relaxation time* (T_1); in a perfect crystal with high nuclear heterogeneity, T_1 dominates $g(\nu)$.

(ii) The *spin-spin interaction time* (T_2) which contributes little to the line width unless the nuclear spin system is relatively homogeneous; NQR experiments deal with imperfect crystal systems, hence additional line width results from

(iii) the statistical distribution of electric field gradients (EFG) caused by crystal inhomogeneities, such as lattice impurities, dislocations and order-disorder effects,

(iv) dislocations and order-disorder effects which are quite significant in *polycrystalline* samples; the RF field has a random orientation relative to the principal EFG axes, giving a distribution of rotation angles of the nuclear magnetization, and

(v) the dynamical motion in crystals and the magnetic (dipole-dipole) interaction between nuclei.

Earlier work [1] showed discrepancies between line widths measured with low power transient self quenched SRO systems [2] with FM detection, and those measured with high power transient pulse-FT systems to generate FID's and spin echoes from ^{14}N nuclei. Therefore the dependence of Δl on RF pulse intensity and pulse period for a range of polycrystalline nitrogen compounds is studied, using a continuous steady-state pulse train consisting of $0.66\,\pi$ pulses with the pulse-FT system.

A continuous steady-state 90° pulse caused the signal function intensity and relaxation to depend on the pulse separation in both polycrystalline and a single crystal of parachloroaniline [3]. An intense RF field significantly narrowed a line by giving a new angular dependence on the direction cosines of the vector r_{ij} connecting spins i and j. This, and most line narrowing studies, and theories [4–10] have considered *multiple pulse sequences* after which the spin echo is averaged. This differs from the continuous steady-state experiment where the FID is averaged after each pulse. If the initial pulse causes narrowing any succeeding pulse will compound the problem.

Experimental

Spectrometers

Two transient spectrometers were used:

(i) Low Power Transient System: a self-quenched SRO with FM detection [2], with two adjustable variables: (a) the peak-to-peak voltage of the RF pulse, (b) the quench period determined by adjustable potentiometers which change the RC time constant of the circuit. T_2^* is measured [2] at the threshold quench frequency [11] between 800 Hz and 3000 Hz depending [2] on the compound and

* Presented at the VIIIth International Symposium on Nuclear Quadrupole Resonance Spectroscopy, Darmstadt, July 22–26, 1985.

Reprint requests to Prof. M. A. Whitehead, Department of Chemistry, McGill University, 801 Sherbrooke St. West, Montréal, Québec, Canada H3A-2K6.

0340-4811 / 86 / 0100-0386 $ 01.30/0. – Please order a reprint rather than making your own copy.

Table 1. Experimental parameters in the high power transient methods.

					R.F. power study			Pulse separation study		
Cmpd.	Temp. (K)	Line	Resonance frequency (MHz)	Pulse frequency (MHz)	Pulse width (μs)	Pulse separation (ms)	R.M.S. power range (w)	R.M.S. power (w)	Pulse width (μs)	Pulse separation range (s)
HMT	296	ν_0	3.3055	3.3060	10,50	20,200	40–5000	110	65.2	0.00005–10.0
	77	ν_0	3.4060	3.4150	20	20 000	40–4200	400	20	0.2–60.0
$NaNO_2$	296	ν_+	4.642	4.612	20	300	40–5000	898	45.0	0.001–10
		ν_-	3.539	3.604	40	200	40–5000	898	53.0	0.001–10
	77	ν_+	4.880							
		ν_-	3.769	3.750	60	60 000	40–4200	400	60	0.06–60.0
$4CH_3O-C_6H_4NH_2$	296	ν_+	3.2860	3.2730	60	300	40–5000			
		ν_-	2.7220	2.7233	60	300	40–5000			
	77	ν_+	3.2442	3.2464	25	200	40–4200			
		ν_-	2.8854	2.8800	40	500	40–4200	1600	40	0.00005–50
BrCN	296	ν_+	2.4650	2.4600	50	500	40–5000			
		ν_-	2.4627	2.4600	50	500	40–5000			
	77	ν_+	2.5203	2.51500				1600	40	0.1–100
		ν_-	2.5109	2.51500				1600	40	0.1–100
$4NH_2-C_6H_4CN$ *	296	ν_+	2.9115	2.9120	50	250	40–5000			
		ν_-	2.5730	2.5840	50	250	40–5000			
	77	ν_+	N/A	N/A	N/A	N/A	N/A	N/A	N/A	N/A
		ν_-	N/A	N/A	N/A	N/A	N/A	N/A	N/A	N/A

* only 4 CN studied to date.

the circuit Q. The RMS power per RF pulse was 0.10 W yielding an RF pulse energy of 10^{-6} J and a pulse field strength of 4 G.

(ii) A High Power Transient System: this pulse-FT system [1] evaluated the continuous steady-state FID from "90°" pulses (0.66 π). The variables were the peak-to peak voltage and separation. The RMS power per pulse was 40 W to 5000 W, corresponding to a pulse field strength of 25 G to 260 G. Table I contains the experimental parameters for each compound. The time averaged pulse energy, $\bar{E}$, and the energy per pulse, E, were calculated [5] with the data in Table 1.

Temperature

The RF coil was immersed in a paraffin oil bath at room temperature because the high RF power heats the sample by 1.7 K in an hour. With the paraffin oil bath the temperature increase in an hour was less than 0.1 K. Stirring the oil eliminated even this increase to within the limits of accuracy (0.05 K).

No temperature variation in the sample was detected with the sample in liquid nitrogen (77 K).

Compounds

The compounds were: Hexamethylenetetramine (HMT), Bromocyanogen (BrCN), 4-Aminobenzonitrile ($4\text{-}NH_2C_6H_4CN$), 4-Methoxyaniline ($4\text{-}CH_3OC_6H_4NH_2$), and Sodium Nitrite ($NaNO_2$). They were ground, dried in a desicator, and ampouled in a 15 mm o.d. pyrex test tube under dry nitrogen gas. All compounds were 99+% pure with exception of $4\text{-}CH_3OC_6H_4NH_2$ at 97+%.

Information about the mass of each sample and the total number of ^{14}N nuclei available for irradiation is given in Table 2.

Calculations

The distribution of nuclear spins at thermal equilibrium is described by a Boltzman term for each level [12] and the difference in population between any two spin states is then

$$\Delta N_{ij} = N_i - N_j = \{2/(2I+1)\} \cdot N_T[\exp(-E_i/kT) - \exp(-E_j/kT)], \quad (1)$$

where $N_T = N_i + N_j$.

Table 2. Sample, energy, and magnetic detail about the ^{14}N compound studied.

Compound				T (K)	η	ν (MHz)	Max energy capacity ($T_2^* = \infty$)		Magn. field strength for max. S/N		
Name	GMW (g/mol)	Mass (g)	# ^{14}N Nucl. (10^{22})				ΔN (10^{16})	E_{max} (10^{-11} J)	T_1 (s)	T_2^* (μs)	H_1[a] (G)
HMT	140	10	17.2	296	0	3.306	6.15	6.75	0.01	673	0.1
				77	0	3.407	36.6	41.2	17	1400	0.002
				296	0.001	2.465	0.909	0.74	0.5	1020	0.004
						2.463	0.909	0.74	0.5	1020	0.004
BrCN	106	6	3.41	77	0.006	2.520	5.36	2.98	N/A[b]	N/A	N/A
						2.511	5.34	2.96	N/A	N/A	N/A
$4NH_2C_6H_4-CN$ *	118	10	5.10	296	0.18	2.912	1.61	1.56	N/A	630	N/A
						2.573	1.42	1.21	N/A	640	N/A
$4CH_3O-C_6H_4NH_2$	123	8	3.92	296	0.28	3.286	1.39	1.52	0.003	230	0.3
						2.722	1.15	1.04	0.011	1500	0.3
				77	0.18	3.244	5.28	5.70	N/A	802	N/A
						2.885	4.80	4.49	N/A	725	N/A
$NaNO_2$	70	10	8.60	296	0.38	4.642	4.32	6.60	0.09	595	0.2
						3.539	3.29	3.86	0.20	725	0.3
				77	0.40	4.880	17.5	28.3	5	378	0.002
						3.769	13.5	11.2	60	517	0.002

[a] $H_1 = 1/\gamma[T_1 T_2^* (I+M)(I-M+1)]^{-1/2}$. [b] N/A = not available. * only CN studied to date.

Table 3. Results of linewidth measurement, Δl, and narrowing, $\Delta(\Delta l)$.

Cmpd.	T	η	line	Pulse energy (J) = E			Time AVG pulse energy (J/s) = $\bar{E}$		
				Δl intercept (Hz)		$\Delta(\Delta l)$ Hz	Δl intercept (Hz)		$\Delta(\Delta l)$ Hz
				Rapid narrowing	Slow narrowing		Rapid narrowing	Slow narrowing	
HMT	296	0	ν_0	753	752	1	770	750	20
	77	0	ν_0	629	684	55	620	720	100
BrCN	296	0.001	ν_+	487	412	75	506	414	92
			ν_-	492	418	74	483	418	65
	77	0.006	ν_+				360	340	20
			ν_-				372	370	2
$4NH_2C_6H_4-CN$ *	296	0.18	ν_+	634	435	199	634	458	176
			ν_-	632	537	95	632	544	90
$4CH_3O-C_6H_4NH_2$	296	0.28	ν_+	2314	323	1991	2740	323	2420
			ν_-	3631	381	3250	3968	328	3640
	77	0.18	ν_+						
			ν_-	800	740	60	718	600	118
$NaNO_2$	296	0.38	ν_+	787	445	342	817	458	367
			ν_-	670	315	355	592	315	277
	77	0.40	ν_+						
			ν_-	883	729	154	790	786	4

* only CN studied to date.

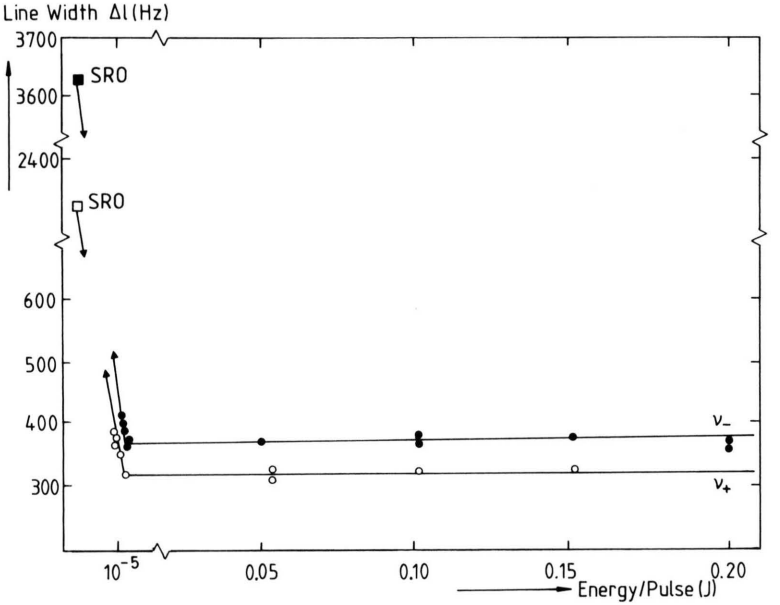

Fig. 1. Dependence of the line width on the energy per pulse of irradiation (J) for 4-$CH_3OC_6H_4NH_2$ at 296 K. Solid circles and squares: ν_- line; open circles and squares: ν_+ line; squares: SRO results.

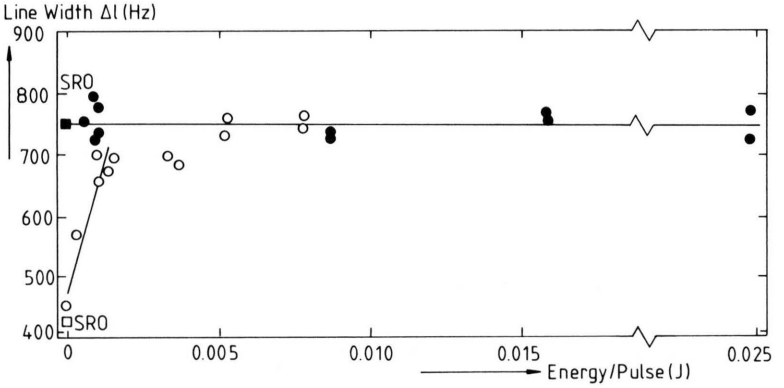

Fig. 3. Dependence of the line width on the energy per pulse of irradiation (J) for HMT at 296 K solid circles, and 77 K open circles. Note that the squares are for the SRO results measured at threshold quench frequency. Not all the data used in the regression analysis are shown.

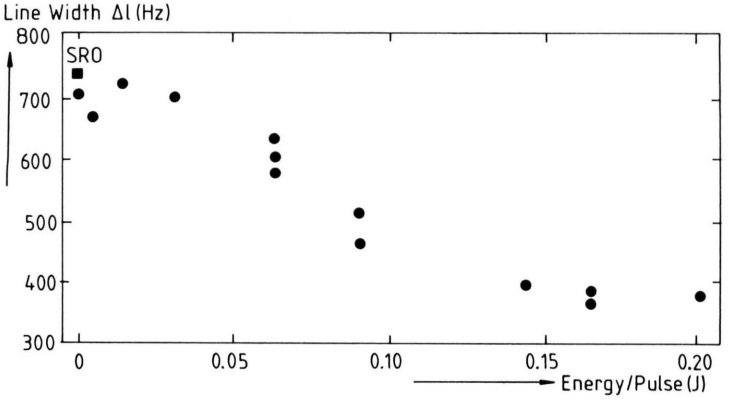

Fig. 2. Dependence of the line width on the energy per pulse of irradiation (J) for 4-$CH_3OC_6H_4NH_2$ at 77 K. Solid circles and squares: ν_- line; square: SRO result.

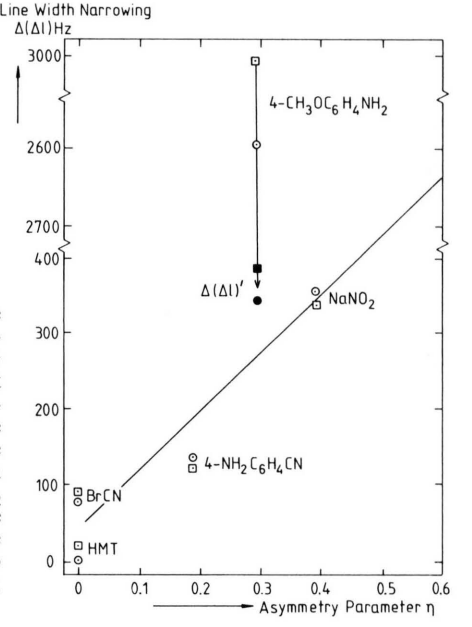

Fig. 4. Dependence of the average line width narrowing $\Delta(\Delta l)$ on the EFG asymmetry parameter η at 296 K. Open Circles: average RF energy per pulse data; open squares: time average RF energy data [12]. The 4-$CH_3OC_6H_4NH_2$ solid points approach the line when the dipole-dipole second moment is used to scale the narrowing from the open points.

If an excited nucleus does not relax (i.e. the inverse line width parameter $T_2^* = \infty$) the maximum energy absorption is

$$E_{max} = 1/2\,(E_i - E_j)\,\Delta N_{ij} \quad (2)$$

$$= 1/2\,h\nu_{ij}\Delta N_{ij}\,, \quad (3)$$

where ν_{ij} is the RF causing a transition from level j to level i. The calculated ΔN and E_{max} are given in Table II.

Excited nuclear spins relax by the mechanisms given in the introduction. For a regenerative oscillator the maximum signal to noise ratio (S/N) for ^{14}N for $I = 1$ occurs at the condition [13]

$$\gamma_N^2 H_1^2 T_1 T_2^* (2 + m - m^2) = 1\,, \quad (4)$$

where H_1 is the magnetic field due to the RF, γ_N the gyromagnetic ratio for nitrogen = 1936 Hz/G, and m the spin quantum number of the lower state. When the l.h.s. of (4) exceeds 1, the system saturates. The local optimum fields at each ^{14}N nucleus for the compounds evaluated are given in Table 2.

Results

Figures 1 to 3 present the dependence of Δl on the pulse energy for 4-$CH_3OC_6H_4NH_2$ and HMT at 296 K and 77 K. For $NaNO_2$ see reference [12]. A "rapid" narrowing zone at low energies and a "slow" or limited narrowing zone at higher energies is observed for all compounds.

A least squares linear regression on the data of each zone allowed the difference between the vertical intercept of the "rapid" narrowing zone and the "slow" narrowing zone to be calculated; it is called the narrowing parameter, $\Delta(\Delta l)$. These vertical intercepts correspond to the line width of the *unperturbed system* where the RF energy is zero. The intercepts and the $\Delta(\Delta l)$ for each compound are given in Table 3.

Discussion

The compounds range in asymmetry parameter, η, from 0 to 0.40. Figure 4 shows the average $\Delta(\Delta l)$ for each compound as a function of η. Decreased EFG symmetry, or increased η, increases the line width narrowing. This dependence is linear, except for 4-$CH_3OC_6H_4NH_2$. The total line width is given by

$$\Delta l(T) = \Delta l(\text{dipolar}) + \Delta l(\text{electric}) + \Delta l(\text{dynamic})\,. \quad (5)$$

The intense RF field only couples with the Δl(dip.), and the trends in the line width should reflect Δl(dip.) even though Δl(el.) and Δl(dyn.) contribute.

Intense RF irradiation gives a new angular dependence to the direction cosines α_{ij}, β_{ij}, and γ_{ij} of the vector r_{ij} connecting the spins i and j. This angular dependence $(\alpha_{ij}^2 - \beta_{ij}^2)^2$ does not occur in the ordinary dipolar second moment of NQR lines, and it considerably reduces the dipolar second moment contribution to the line width [14]. The line width narrowing with RF power is therefore caused by this effect.

The calculations were for a cubic lattice site. In a system of high η, the site will be far from cubic. The term $(\alpha_{ij}^2 - \beta_{ij}^2)^2$ consequently becomes larger, reducing the dipolar second moment which gives the observed dependence of line narrowing with RF power on η.

The experimental narrowing of 4-$CH_3OC_6H_4NH_2$ occurs because it has the largest dipolar line width contribution by the hydrogen bonded to nitrogen in the NH_2 group with an N–H bond length of 1.08 Å. In a perfect crystal of HMT the intermolecular dipole line width contribution caused by each hydrogen atom nearest to the nitrogen and 2.08 Å away is [15] $\langle \Delta\nu_i^2 \rangle = 2370\,Hz^2$. The second moment contributions vary as r^{-6}, hence in $CH_3OC_6H_4NH_2$ the contribution will be 8 times that in HMT. Therefore the term $(\alpha_{ij}^2 - \beta_{ij}^2)^2$ causes a very great decrease in the dipolar second moment contribution to the line width for large dipolar coupling. If the result for 4-$CH_3OC_6H_4NH_2$ is divided by 8, the narrowing observed falls in the region for the other compounds, $\Delta(\Delta l)'$. Thus at room temperature $(\alpha_{ij}^2 - \beta_{ij}^2)^2$ reduces almost to zero the contribution of the dipolar second moment to the line width. In the SRO result with weak RF power the full second moment contribution to the line width occurs.

Experimentally the line width narrows rapidly with RF power and, after an RF power characteristic of the chemical compound, slowly narrows with increasing RF power. This suggests that the $(\alpha_{ij}^2 - \beta_{ij}^2)^2$ term reaches a maximum with RF power.

At liquid nitrogen, HMT shows line broadening and $\Delta(\Delta l)$ is negative; for 4-$CH_3OC_6H_4NH_2$, $\Delta(\Delta l)$ is still slightly positive and narrows by a similar amount as for $NaNO_2$ and BrCN. However, 4-$CH_3OC_6H_4NH_2$ has a different crystal structure at 77 K, with a phase change at [1] 244 K. The NH_2 group now lies in a single low energy minimum [1] rather than in the room temperature double minimum. At 77 K the structure has a larger EFG because the NH_2 group is planar and it has a more-symmetric environment [1]. Therefore less reduction in the line width occurs due to the dipolar second moment. It will still exceed that in HMT which has a very symmetric structure and is tightly bound [15].

The Δl(dip.) calculations for HMT were for a pure single crystal, and it was assumed that Δl(el.) was zero. The line width is therefore maximal for Δl(dip.). As the grain boundaries, dislocations and impurities are included, Δl(dip.) decreases since less interactions are possible while Δl(el.) increases as will Δl(dyn.). Calculations of these inter-related effects will be necessary to give an unambiguous interpretation of the present results. Δl(el.) can vary dramatically with temperature and phase [16], while Δl(dyn.) is also strongly temperature dependent.

The dependence of $\Delta(\Delta l)$ on pulse separation, τ, was found to be quite small. When $\tau > T_1$, $\Delta(\Delta l)$ was fully described by the pulse energy alone. Only when $\tau < T_2^*$ did some narrowing occur [10], which was more effectively described by the time averaged energy, $\bar{E}$. For $NaNO_2$ with a weak pulse of 0.4 mJ the narrowing obtained when $\tau < T_2^*$ was about 12%. As the pulse energy was increased the line width remained narrowed regardless of how large τ became. Consequently, for a continuous steady-state pulse experiment, where the FID is averaged, the RF power dominates the line narrowing effect.

The RF energy per pulse in the pulse-FT system is 10^3 to 10^6 times greater than in the SRO. The pulse energy capacity and optimum magnetic field strength for the ^{14}N nuclei of each compound (Table 2) show that high power transient systems should be operated with the narrowest pulse width and lowest possible RF power to detect signals. Small changes in pulse energy give data for a linear regression to zero pulse energy.

Conclusion

In ^{14}N NQR pulse spectrometer studies the initial pulse fully determines the subsequent measured line widths and line width parameters. The line frequencies are in no way affected. Unless the first pulse is fully defined and the line width recorded, any subsequent changes in line width caused by additional pulses become arbitrary [3–10, 14]. An unperturbed line width would be measured at zero RF field. If the results at low pulse power are projected back through the SRO result, an approximate zero RF power line width may be obtained, which may be useful in relating different pulse-spectrometers studies.

Acknowledgements

This research was supported by the NSERC (Canada). RJT is grateful to CIP Ltd. for help and encouragement. The referee is thanked for useful criticism.

[1] R. J. Trepanier and M. A. Whitehead, J. Mol. Struct. **111,** 415 (1983).
[2] R. J. Trepanier and M. A. Whitehead, J. Mol. Struct. **83,** 369 (1982).
[3] S. Vega, J. Chem. Phys. **63,** 3770 (1975).
[4] T. Ito and T. Hashi, J. Mol. Struct. **58,** 389 (1980).
[5] D. Ya. Osokin, J. Mol. Struct. **83,** 243 (1982).
[6] O. S. Zueva and A. R. Kessel, J. Mol. Struct. **83,** 383 (1982).
[7] J. C. Pratt, J. Mol. Struct. **111,** 113 (1983).
[8] A. E. Mefed and B. N. Pavlov, J. Mol. Struct. **83,** 131 (1982).
[9] R. A. Marino and S. M. Klainer, J. Chem. Phys. **67,** 3388 (1977). D. Ya. Osokin, Phys. Sta. Sol (b), **102,** 681 (1980). O. S. Zueva, J. Mol. Struct. **83,** 379 (1982).
[10] K. P. Dinse, RAMIS 85, Proceedings of the Conference, Radio and Microwave Spectroscopy, Dymaczewo, Poland 1985, pp. 167–180.
[11] S. Melnick, R. J. Trepanier, M. A. Whitehead, and E. P. A. Sullivan, J. Mol. Struct. **58,** 337 (1980).
[12] R. J. Trepanier and M. A. Whitehead, RAMIS 85, Proceedings of the Conference, Radio and Microwave Spectroscopy, Dymaczewo, Poland 1985, pp. 181–189.
[13] T. P. Das and E. L. Hahn, Nuclear Quadrupole Resonance Spectroscopy, Academic Press, New York 1958, p. 60.
[14] A. R. Kessel and O. S. Zueva, Phys. Lett. **68A,** 347 (1978).
[15] R. J. Trepanier and M. A. Whitehead, J. Chem. Soc. Faraday Trans. II, **82** (1986), in press.
[16] S. J. Melnick and M. A. Whitehead, J. Mol. Struct. **111,** 397 (1983).